How to cite: Angew. Chem. Int. Ed. 2024, e202407805
doi.org/10.1002/anie.202407805

Host-Guest Systems Hot Paper

1,3,5–2,4,6-Functionalized Benzene Molecular Cage: An Environmentally Responsive Scaffold that Supports Hierarchical Superstructures

Xin-Yu Pang, Hang Zhou, Xiaojiang Xie, Wei Jiang, Yinhua Yang, Jonathan L. Sessler, and Han-Yuan Gong**

In memory of Professor Wei Jiang.

Abstract: New stimulus-responsive scaffolds are of interest as constituents of hierarchical supramolecular ensembles. 1,3,5–2,4,6-Functionalized, facially segregated benzene moieties have a time-honored role as building blocks for host molecules. However, their user as switchable motifs in the construction of multi-component supramolecular structures remains poorly explored. Here, we report a molecular cage **1**, which consists of a bent anthracene dimer **3** paired with 1,3,5-tris(aminomethyl)-2,4,6-triethylbenzene **2**. As the result of the pH-induced *ababab*↔*bababa* isomerization of the constituent-functionalized benzene units derived from **2**, this cage can reversibly convert between an open state and a closed form, both in solution and in the solid state. Cage **1** was used to create stimuli-responsive hierarchical superstructures, namely Russian doll-like complexes with $[K\subset 18\text{-crown-}6\subset \mathbf{1}]^+$ and $[K\subset \text{cryptand-}222\subset \mathbf{1}]^+$. The reversible assembly and disassembly of these superstructures could be induced by switching cage **1** from its open to closed form. The present study thus provides an unusual example where pH-triggered conformation motion within a cage-like scaffold is used to control the formation and disassociation of hierarchical ensembles.

Introduction

To date, a number of artificial stimuli-responsive hosts have been developed[1] with the resulting systems attracting attention in areas as diverse as molecular switching,[2] catalysis,[3] and separation.[4] In contrast, stimuli-responsive hosts have not been exploited extensively to create multi-component or hierarchical supramolecular ensembles whose assembly and disassembly can be readily controlled.[5] Here we report a molecular cage **1** based on a 1,3,5–2,4,6-functionalized, facially segregated benzene core that acts as a switchable motif and which supports the controlled assembly and disassembly of Russian doll-like host–guest complexes with $[K\subset 18\text{-crown-}6]^+$ and $[K\subset \text{cryptand-}222]^+$.

1,3,5–2,4,6-Functionalized, facially segregated benzenes are a special family of hexasubstituted benzenes. They can adopt a stable *ababab* (or *bababa*) configuration with six substituents alternately positioned above (*a*) and below (*b*) the benzene plane (Scheme 1).[6] These benzene derivatives have been widely employed as building blocks to create preorganized host molecules.[7–9] However, despite the development of more than 500 hosts based on hexasubstituted benzenes since the first such structure was reported in 1993,[9d,10] to our knowledge, these cores have yet to be exploited as stimulus-responsive scaffolds within larger supramolecular constructs. Cage **1** retains the pH-induced *ababab*↔*bababa* isomerization of hexasubstituted benzenes and undergoes reversible transitions between limiting open (*out,out* conformation) and closed (*in,in* conformation) states.

As detailed below, the open form of cage **1** binds $[K\subset 18\text{-crown-}6]^+$ and $[K\subset \text{cryptand-}222]^+$ to form Russian doll-like multi-component ensembles where the K^+ acts as the inner "doll", while the crown/cryptand and receptor **1** act as the 2nd and 3rd doll layers, respectively. In the presence of acid, the structural conformation of the constituent cage undergoes a transformation from an open to closed state, promoting expulsion of the bound potassium cation-containing guest. Adding base induces rebinding of the guest. This study extends the utility of hexasubstituted benzene motifs

[*] X.-Y. Pang, Prof. Dr. X. Xie, Prof. Dr. W. Jiang, Dr. Y. Yang
Department of Chemistry
Southern University of Science and Technology
Shenzhen 518055, P. R. China
Prof. Dr. H.-Y. Gong
College of Chemistry
Beijing Normal University
Beijing 100875, P. R. China
E-mail: hanyuangong@bnu.edu.cn
Prof. Dr. J. L. Sessler
College of Chemistry
The University of Texas at Austin
Austin, Texas 78712-1224, United States
E-mail: sessler@cm.utexas.edu
H. Zhou
Department of Chemistry
The University of Hong Kong
Hong Kong, P. R. China

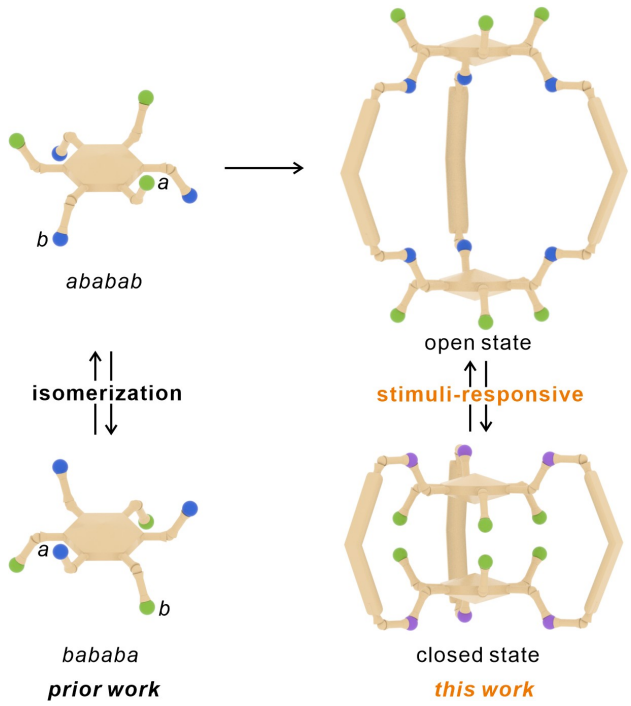

Scheme 1. Schematic representation of the interconversion between the two most stable conformations of hexasubstituted benzenes (*ababab* and *bababa*) and the stimuli-driven reversible structural changes between the open and closed forms of cage **1**.

beyond their conventional role as building blocks for elaborated hosts, while highlighting a new strategy for creating self-assembled stimuli-responsive hierarchical materials.

Results and Discussion

Design, Synthesis, and Characterization of Cage 1

Cage **1**, was prepared by first mixing 1,3,5-tris(aminomethyl)-2,4,6-triethylbenzene **2** and the bent aldehyde-functionalized anthracene dimer **3** (Scheme 2a) in a 2:3 ratio and stirring for 12 h in dry dichloromethane. Following this imine bond-forming step, sodium borohydride reduction in situ gave cage **1** in 87 % yield. Taking into account all the synthetic steps starting from commercially available materials, the overall yield of cage **1** is 48 %. NMR spectral studies and high-resolution mass spectrometric (HR-MS) analyses provided support for the proposed structure (see Supporting Information, Figures S1–S5). In cage **1**, the benzene "panels" derived from **2** serve as the "roof" and "floor", respectively, while the amine groups serve as putative stimuli-responsive moieties. The anthracene subunits of **3** act as "side walls", while providing large π surfaces that were expected to support host–guest interactions.[11,12] The well-defined cavity present in cage **1** (calculated to be ca. 730 Å^3) was expected to accommodate appropriately sized guest molecules that could presumably enter and exit through the aperture between two neighboring side walls (Scheme 2b).

Single crystals of cage **1** suitable for X-ray diffraction analysis were obtained by slow evaporation of a toluene solution. Relative to its calculated optimized geometry, in the solid-state cage **1** is distorted in a way that serves to enlarge its aperture but decrease its apparent volume (Figure 1). For instance, the cavity height of **1** is 17.2 Å. This value is 1.5 Å greater than in the optimized structure. On the other hand, the estimated cavity volume is 328 Å^3, which constitutes a 55 % reduction relative to the optimized structure. Neighboring cage molecules exhibit an antiparallel stacking arrangement with toluene solvent molecules located within the interstitial spaces between adjacent hosts (Figure S6).

Solid-State Behavior of Cage 1

The impact of secondary amine protonation on cage **1** was explored in the presence of trifluoroacetic acid (TFA). Single crystals of the fully protonated form of **1** ($[\mathbf{1}+6H]^{6+}\cdot 6CF_3COO^-$) were obtained via the gradual evaporation of a solution of cage **1** in THF and CH_3OH containing an excess

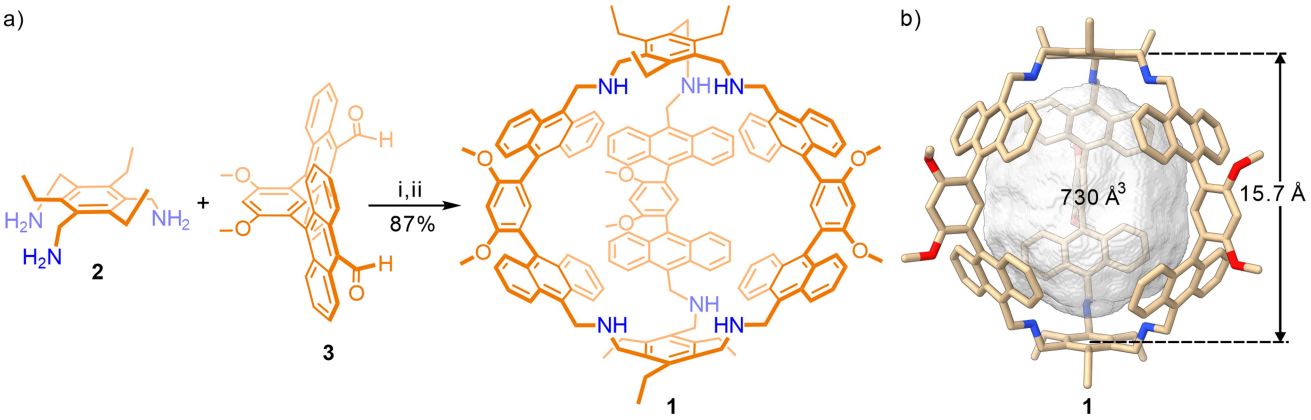

Scheme 2. (a) Synthesis[a] and (b) DFT optimized structure of molecular cage **1**. [a] Experimental conditions: (i) Dry CH_2Cl_2, RT, 12 h; (ii) $NaBH_4$, RT, 3 h.

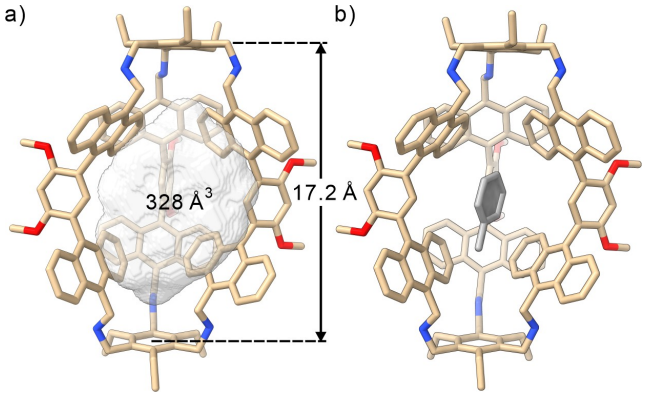

Figure 1. Single-crystal structure of toluene⊂**1**: (a) Cavity size and (b) side view. Hydrogen atoms and solvent molecules have been omitted for clarity.

of TFA. The resulting crystallographic analysis revealed that cage **1** underwent a substantial conformational change upon protonation. Specifically the *out,out*-conformation seen in the neutral form, (*out,out*-**1**) an open state with an *ababab* arrangement of the ethyl groups, is transformed to a corresponding *in,in* conformation (in^{3+},in^{3+}-[**1**+6H]).In this closed form, one of the ethyl groups adopts a *bababa* arrangement and the bridging groups ($–CH_2–NH_2^+–CH_2–$) lie outside the cavity. Salt bridges are observed between the secondary ammonium (NH_2^+) centers and the six external CF_3COO^- anions (Figures 2a and 2b). Inversion of the two benzene moieties and the associated six substituents results in constriction of the cavity. This leads to the observed *in,in* conformation (in^{3+},in^{3+}-[**1**+6H]) and stabilization of the closed form. The cavity volume was found to be only 57 Å^3 (as shown in Figure 2c). This represents just 7 % of the volume of that seen in *out,out*-**1**. The result is a host that appears too small to accommodate classic small guests such as benzene.

Separately, a diffraction grade single crystal of in^{3+},out^{3+}-[**1**+6H]·6CF_3COO^- containing two protonated conformers was obtained by subjecting a solution of cage **1** in THF to slow evaporation in the presence of excess TFA (Figure 2d). Analysis of the resulting crystal structure revealed that one hexasubstituted benzene unit adopts exclusively an *in* conformation. A 52 % occupancy for the *out* conformation and 48 % occupancy for the *in* conformation was seen for the other subunit. In spite of the mixed occupancy, this structural analysis was taken as prima facie evidence for the existence of an in^{3+},out^{3+}-[**1**+6H] conformer. In this latter form, three ethyl groups are positioned external to the cavity, while the remaining three ethyl groups point towards the interior of the cavity (Figure 2e). In this conformer, the cavity has a height of 10.3 Å and a volume of 230 Å^3 (Figure 2f). It is noted that the dimensions of the cavity in the in^{3+},out^{3+}-[**1**+6H] conformer are intermediate between what is seen in in^{3+},in^{3+}-[**1**+6H] and *out,out*-**1**.

The differences in the two structures above are translated into the binding sites for the CF_3COO^- counter anions. In in^{3+},in^{3+}-[**1**+6H]·6CF_3COO^-, six CF_3COO^- are positioned outside the cavity, effectively decreasing the electrostatic repulsion between each individual acetate anion. In in^{3+},out^{3+}-[**1**+6H]·6CF_3COO^-, three CF_3COO^- anions form salt bridges with the internally oriented NH_2^+ groups. The remaining three CF_3COO^- anions are found outside the cavity and form salt bridges with outward-pointing NH_2^+ groups.

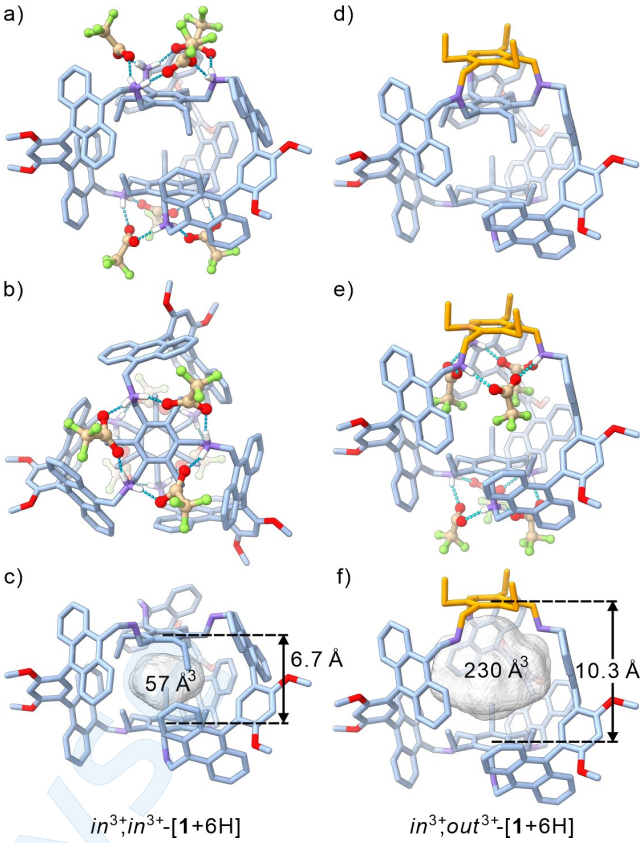

Figure 2. Side (a) and top (b) views, as well as calculations of the cavity size, of **1** (c) from a single-crystal diffraction analysis of in^{3+},in^{3+}-[**1**+6H]·6CF_3COO^-. (d) Single-crystal structure of a mixed system containing two protonated conformers. (e) Side view and (f) the cavity size of the single-crystal structure of in^{3+},out^{3+}-[**1**+6H] ·6CF_3COO^-. Some of the hydrogen atoms and counterions are omitted for clarity.

Solution Phase Behavior of Cage 1

Unknown from the solid state study was whether the *in,in* or *in,out* forms of $[\mathbf{1}+6H]^{6+}$ would prove more stable in solution. An effort was thus made to probe the relative stabilities of **1** and its salt forms in solution. Accordingly, the features of cage **1** were further investigated in CH_2Cl_2 solution. The ^{1}H NMR spectrum (Figure 3a) of neutral cage **1** is consistent with a highly symmetrical (D_{3h}) structure. The signals of H10 and H11 on the ethyl groups of cage **1** are observed at 3.22 and 1.47 ppm, respectively. These values are close to those in other reported cages created using **2** as the building block.[6b,8] This is taken as evidence that the ethyl groups are located outside of the

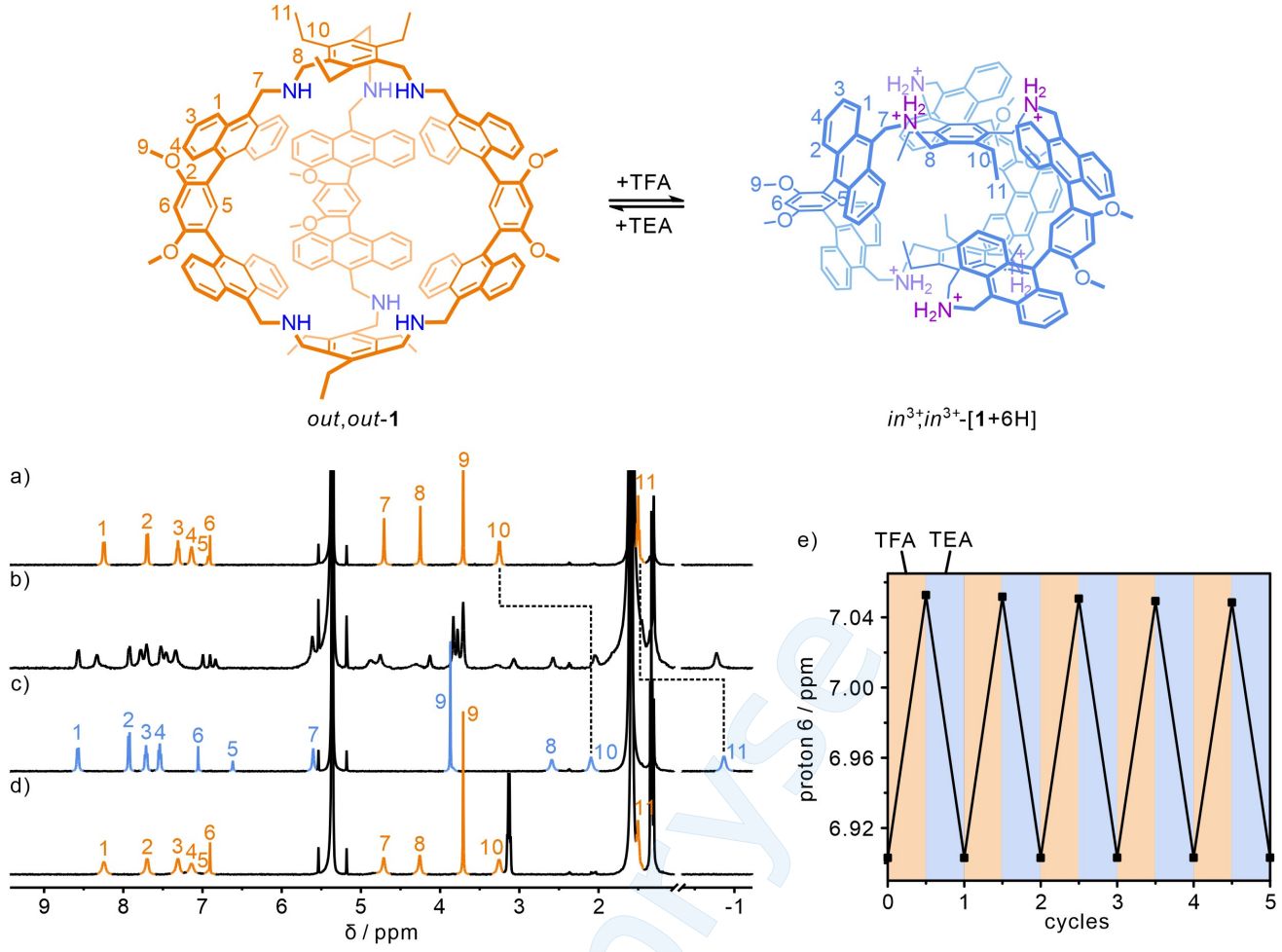

Figure 3. ^{1}H NMR spectra (500 MHz, CD_2Cl_2) of cage **1** recorded in the absence (a) and presence (b) of 3 molar equiv. of TFA, after the further addition of 5 molar equiv. of TFA (c), and the subsequent addition (d) of triethylamine (TEA) (8 molar equiv.). Chemical shift changes in the signal for H6 of cage **1** seen upon alternating additions of TFA and TEA (e). NB: equiv. are relative to **1**.

cavity and thus that the neutral form of cage **1** adopts the *out*,*out* conformation in solution as seen in the solid state.

The effect of protonation on the solution state structure of cage **1** was next investigated by adding gradually TFA to a solution of cage **1** in CD_2Cl_2. Early on in the course of this addition, the ^{1}H NMR signals of **1** were found to be split in a complicated manner. This finding is interpreted in terms of **1** undergoing a conformational change on the NMR time-scale (Figures 3b and S7). The ^{1}H DOSY spectrum of the partially protonated form of **1** was also recorded in CD_2Cl_2. It provides evidence for the existence of a time-averaged species with a diffusion coefficient (D) of 3.53×10^{-9} $m^2\cdot s^{-1}$ (Figure S8).

The proton signals in the ^{1}H NMR spectrum (cf. Figure S9) could not be analyzed readily as a linear combination of signals from in^{3+},in^{3+}-[**1**+6H] and *out*,*out*-**1**. Rather, the spectrum could be divided into three apparent contributions. One contribution consists of signals ascribed to H5 and H6, whose chemical shifts are different from those in in^{3+},in^{3+}-[**1**+6H] and *out*,*out*-**1**. A second set of features closely resemble those of in^{3+},in^{3+}-[**1**+6H], leading us to suggest that one hexasubstituted benzene moiety adopts an in^{3+} conformation upon protonation. The third contribution resembles the spectrum of *out*,*out*-**1**, albeit with a slight downfield shift. This was taken as an indication that one hexasubstituted benzene adopts an *out* conformation. The underlying spectral assignments were made on the basis of a 2D ROESY spectral analysis (Figure S10). Taken in concert, therefore, these observations provide support for notion that initial protonation leads to the emergence of a new species, in^{3+},*out*-[**1**+3H], that incorporates both in^{3+} and *out* conformations.

The further addition of TFA to the above solution led to a rather simple ^{1}H NMR spectrum (Figure 3c). This spectrum did not change as further equiv. of TFA were added, leading us to infer that **1** becomes fully protonated in the presence of excess TFA. This protonated form was characterized by a spectrum in which the majority of the proton signals were shifted to lower field relative to **1**, while the signals of H10 and H11 on the ethyl groups exhibited large upfield shifts. This observation is rationalized in terms of the electron-rich anthracene sidewalls serving to shield ethyl groups.

A correlation between the signals H11 and H5 was observed in both the 2D and 1D ROESY spectra recorded after the addition of excess TFA (Figures S11–S13). The finding supports the contention that the fully protonated form of cage **1** adopts the *in,in* conformation in CD_2Cl_2 solution. The conformational change from *out,out* to *in,in* seen upon protonation was recapitulated in other solvents, such as CD_2Cl_2/CD_3CN (1:1, *v*/*v*) and THF-d_8 (Figures S14 and S15). This leads us to suggest that the molecular motion seen upon adding TFA reflects protonation, rather than a solvent effect.

It is noteworthy that both conformers (i.e., in^{3+},in^{3+}-[**1**+6H] and in^{3+},out^{3+}-[**1**+6H]) were found in single crystals of the completely protonated cage **1** as discussed above. However, only the former species was observed in solution in the presence of excess TFA. Furthermore, only the *out,out*-**1** conformer was observed for the neutral cage in both solution and the solid state. Theoretical calculations, both in vacuum and using the COSMO solvation model, were carried out using semiempirical methods (PM7) with the MOPAC software.[13] The conformational preferences among all three conformers (i.e., *in,in*, *in,out*, and *out,out*) of the neutral or completely protonated cages were analyzed. On the basis of the results, we conclude that the observed conformers of cage **1** are determined by the corresponding thermodynamic stabilities. In the case of the neutral cage, the *out,out*-**1** conformer is the most stable with interactions between cage **1** and solvent molecules serving to stabilize this conformer. After complete protonation, the in^{3+},in^{3+}-[**1**+6H] conformer has the lowest formation energy. Contributing to this stability is that this form allows the CF_3COO^- counter anions to adopt a more stable arrangement consistent with what is seen in the solid state. The in^{3+},out^{3+}-[**1**+6H] conformer is less stable than the in^{3+},in^{3+}-[**1**+6H] conformer, as might be inferred by its observation only in the solid state (as one of two forms) and not in solution (see Supporting Information, Table S1).

The reversible interconversion between in^{3+},in^{3+}-[**1**+6H] and *out,out*-**1** was then examined. The chemical shifts of the proton signals for **1** returned to their original values after the addition of triethylamine (TEA, 8 molar equiv. relative to **1**) to the solution of in^{3+},in^{3+}-[**1**+6H] produced upon adding a total of 8 equiv. of TFA (Figure 3d). This observation is interpreted in terms of the deprotonation-induced transformation of cage **1** from a closed state to an open state. Adding TFA and TEA in sequence allowed this interconversion process to be repeated through multiple cycles with little if any attenuation (Figures 3e and S16).

Stimuli-Responsive Russian Doll Assemblies

In recent years, hierarchical architectures (including host-in-host[14] and Russian doll assemblies[15]), have attracted considerable interest due to their aesthetics,[16] appealing binding properties,[17] and potential utility in a range of application areas.[18] However, as noted in the introduction, the construction of hierarchical superstructures that display stimuli-response features remains a challenge.[5] The well-defined protonation-mediated switching behavior of cage **1** motivated us to explore its potential to construct stimuli-responsive hierarchical superstructures. The neutral form of cage **1** (existing in the *out,out* conformation) has a relatively large internal cavity. We thus postulated that it would form host–guest complexes with suitably chosen substrates. It was further anticipated that acid-base mediated control over the conformation of cage **1**, specifically its conversion between an open state (*out,out* conformation) and closed state (*in,in* conformation), would allow guest uptake/release to be switched on and off at will. In the case of suitably chosen guests, this process might allow for the controlled assembly and disassembly of hierarchical architectures.

To test these possibilities, crown ether/cryptand-cation complexes were chosen as putative guests (Figure 4a). While crown ether complexes have been encapsulated effectively using various synthetic hosts,[19] there have been limited reports on the stimulus-responsive assembly and disassembly of the resulting ensembles.[20] Furthermore, we are unaware of a cryptand-metal cation complex enclosed within a host that has been characterized via a single crystal X-ray diffraction analysis.

The ensembles [K⊂18-crown-6⊂**1**]$^+$ and [K⊂cryptand-222⊂**1**]$^+$ were investigated first in the solid state. The crystal structure of [K⊂18-crown-6⊂**1**]$^+\cdot PF_6^-$ (Figure 4b) revealed

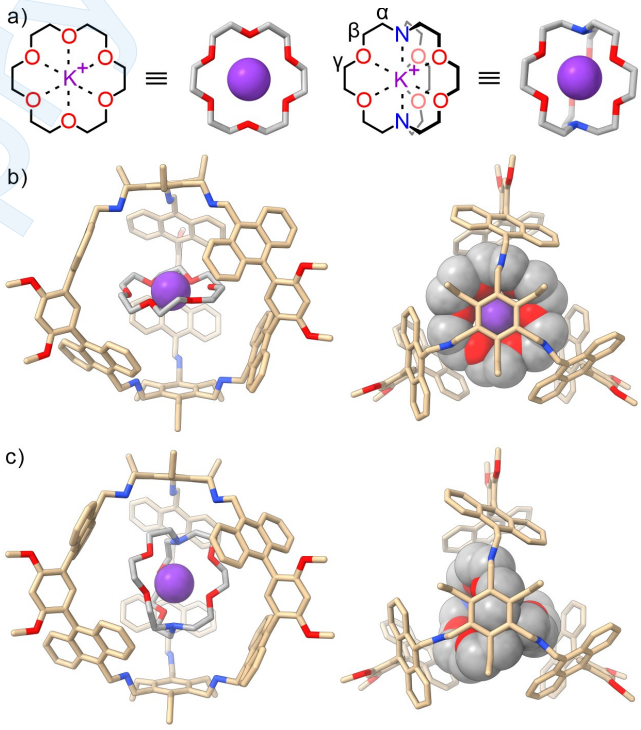

Figure 4. (a) Chemical structures and schematic representations of [K⊂18-crown-6]$^+$ and [K⊂cryptand-222]$^+$. (b) Views of [K⊂18-crown-6⊂**1**]$^+$ and (c) [K⊂cryptand-222⊂**1**]$^+$ seen in the single-crystal structure of [K⊂18-crown-6⊂**1**]$^+\cdot PF_6^-\cdot 5CH_3OH\cdot 5CH_2Cl_2\cdot 3H_2O$ and [K⊂cryptand-222⊂**1**]$^+\cdot PF_6^-\cdot 4CH_3OH\cdot 3CH_2Cl_2$. Hydrogen atoms and counterions are omitted for clarity. The volumes of the cavity of cage **1** in [K⊂18-crown-6]$^+$ and [K⊂cryptand-222]$^+$ (see main text) were calculated based on the corresponding crystal structures.

a Russian doll-like arrangement wherein the cation serves as the first "doll", the crown ether, the second, and cage **1** the third. In this ensemble, the constituent $[K\subset 18\text{-crown-}6]^+$ complex is roughly planar and positioned on the equatorial plane of **1**. In contrast, the PF_6^- counter anion is situated outside the cavity. The calculated volume of $[K\subset 18\text{-crown-}6]^+$ (ca. 273 Å^3) is significantly smaller than that of cage **1** cavity (722 Å^3) (packing coefficient[21] = 0.38). This difference in volume creates two voids within the cavity above and below the enclosed $[K\subset 18\text{-crown-}6]^+$ ion. On the other hand, C–H···π interactions between the CH_2 groups on the 18-crown-6 and the anthracene sidewalls of **1** are inferred from the binding arrangement (Figure S17).

In contrast to what was seen in the case of the $[K\subset 18\text{-crown-}6]^+$ guest, a solid state structural analysis of $[K\subset\text{cryptand-222}\subset\mathbf{1}]^+$ (Figure 4c) revealed that the internal space of cage **1**, with a volume of 742 Å^3 in this crystalline species, is effectively filled with the $[K\subset\text{cryptand-222}]^+$ guest, which occupies a volume of 374 Å^3 (packing coefficient of 0.51). Multiple C–H···π interactions between CH_2 groups on cryptand-222 and anthracene sidewalls of cage **1** are inferred based on the metric parameters (Figure S18). To the best of our knowledge, this represents the first example wherein the inclusion of $[K\subset\text{cryptand-222}]^+$ within the cavity of a discrete host molecule has been confirmed via a single-crystal X-ray diffraction analysis.

The interactions between cage **1** and $[K\subset 18\text{-crown-}6]^+$ were next studied in CD_3CN/CD_2Cl_2 (1:1, *v*/*v*). In the ^{1}H NMR spectrum of a 1:1 mixture of $[K\subset 18\text{-crown-}6]^+$ and **1** (Figure S19), signals ascribed to $[K\subset 18\text{-crown-}6]^+$ were seen that are upfield shifted relative to the free cation complex. Furthermore, a correlation between H5 on cage **1** and the protons of $[K\subset 18\text{-crown-}6]^+$ was observed in the 1D NOE spectrum (Figure S20). The findings provide support for the notion that cage **1** is able to bind the $[K\subset 18\text{-crown-}6]^+$ cation effectively within its cavity in solution, similar to what is seen in the single crystal structure discussed above. Follow-up NMR spectral titrations revealed that cage **1** exhibits a moderate affinity towards $[K\subset 18\text{-crown-}6]^+$ ($K_a = 1.4\times10^3$ M^{-1}) (Figures S21 and S22). Conversely, it displays no appreciable affinity for either the metal-free 18-crown-6 ($K_a = 14$ M^{-1}) or $K^+PF_6^-$ (the corresponding K_a value is too small to determine accurately) (Figures S23–S27).

As expected for a three layer Russian doll assembly containing a K^+ cation, a crown ether, and cage **1**, formation of $[K\subset 18\text{-crown-}6\subset\mathbf{1}]^+$ was observed when cage **1** was mixed with both 18-crown-6 and $K^+PF_6^-$ in a 1:1:1 molar ratio, as inferred from both ^{1}H NMR spectroscopic studies and HR-MS (Figure S28).

The interactions between **1** and $[K\subset\text{cryptand-222}]^+$ were also studied in CD_3CN/CD_2Cl_2 (1:1, *v*/*v*). In the ^{1}H NMR spectrum of a 1:1 mixture containing $[K\subset\text{cryptand-222}]^+$ and **1** (Figures 5a – 5c), the proton signals ascribed to $[K\subset\text{cryptand-222}]^+$ were no longer detectable above the baseline. Additionally, the majority of the proton signals corresponding to **1** were seen to undergo distinctive shifts. These observations are consistent with the cationic complex $[K\subset\text{cryptand-222}]^+$ likely being encapsulated within the cavity of cage **1** and thus being shielded by the aromatic sidewalls. On the basis of a ^{1}H NMR spectral titration, a binding constant of 1.2×10^5 M^{-1} was calculated for the 1:1 equilibrium between $[K\subset\text{cryptand-222}]^+$ and **1** (Figures S29 and S30). Separate ITC titrations yielded a $K_a = 1.6\times10^5$ M^{-1} (Figure S31). In contrast, a significantly reduced value was seen for the interaction between **1** and the free form of cryptand-222 (Figures S32 – S34). This difference in affinity is taken as evidence that a Russian doll-like assembly $[K\subset\text{cryptand-222}\subset\mathbf{1}]^+$ is formed in solution in the presence of all three constituents, namely K^+, cage **1**, and cryptand-222. The thermodynamic parameters ($\Delta H = -10.7$ kJ·mol^{-1}, $-T\Delta S = -19.1$ kJ·mol^{-1}, $\Delta G = -29.8$ kJ·mol^{-1}) derived from the ITC titrations proved consistent with the notion that the binding between cage **1** and $[K\subset\text{cryptand-222}]^+$ is driven by both entropic and enthalpic contributions. In addition, the ensemble $[K\subset\text{cryptand-222}\subset\mathbf{1}]^+$ proved stable in the gas phase, as inferred from the observation of a major peak corresponding to the intact ensemble in HR-MS (Figure S35).

Subsequently, an investigation was carried out to determine the potential modulation of these Russian doll assemblies based on the pH-dependent switching features of cage **1** noted above. Using $[K\subset\text{cryptand-222}\subset\mathbf{1}]^+$ as an example, it was observed that upon the addition of TFA (8 molar equiv. of **1**) to a CD_2Cl_2/CD_3CN (1:1, *v*/*v*) solution of $[K\subset\text{cryptand-222}\subset\mathbf{1}]^+$ (Figure 5d), ^{1}H NMR signals corresponding to the assembly disappeared while those ascribed to free $[K\subset\text{cryptand-222}]^+$ and *in*$^{3+}$,*in*$^{3+}$-[**1**+6H] appeared. This finding is taken as evidence that the addition of TFA to $[K\subset\text{cryptand-222}\subset\mathbf{1}]^+$ leads to expulsion of the $[K\subset\text{cryptand-222}]^+$ guest and is consistent with the solid state studies (vide supra) that revealed that the protonated form ($[\mathbf{1}+6H]^{6+}$) possesses a cavity that is too small to make it an effective host.

When the solution produced by adding 8 molar equiv. of TFA to $[K\subset\text{cryptand-222}\subset\mathbf{1}]^+$ was treated with tetramethylammonium hydroxide (TMA^+OH^-; 8 molar equiv. relative to **1**) the proton signals corresponding $[K\subset\text{cryptand-222}\subset\mathbf{1}]^+$ reemerged (Figure 5e). Conversely, those for $[K\subset\text{cryptand-222}]^+$ could no longer be observed. On this basis we conclude that re-encapsulation of $[K\subset\text{cryptand-222}]^+$ had taken place. The ^{1}H NMR spectra displayed reversible release and uptake processes when TFA and TMA^+OH^- were added in an alternating manner through multiple cycles (Figures 5f and S36). Similar switchable guest release and re-capture was also confirmed in the case of $[K\subset 18\text{-crown-}6\subset\mathbf{1}]^+$ (Figures S37 and S38).

Conclusions

In summary, we have shown that a 1,3,5–2,4,6-functionalized, facially segregated benzene can be used to create a stimulus-responsive host. This host, cage **1**, can be interconverted between open and closed forms through the pH-induced *ababab*↔*bababa* isomerization of the constituent hexasubstituted benzenes. The neutral, open form of cage **1** was found to be an effective receptor for representative metal-containing crown ethers and cryptands ([K⊂18-crown-

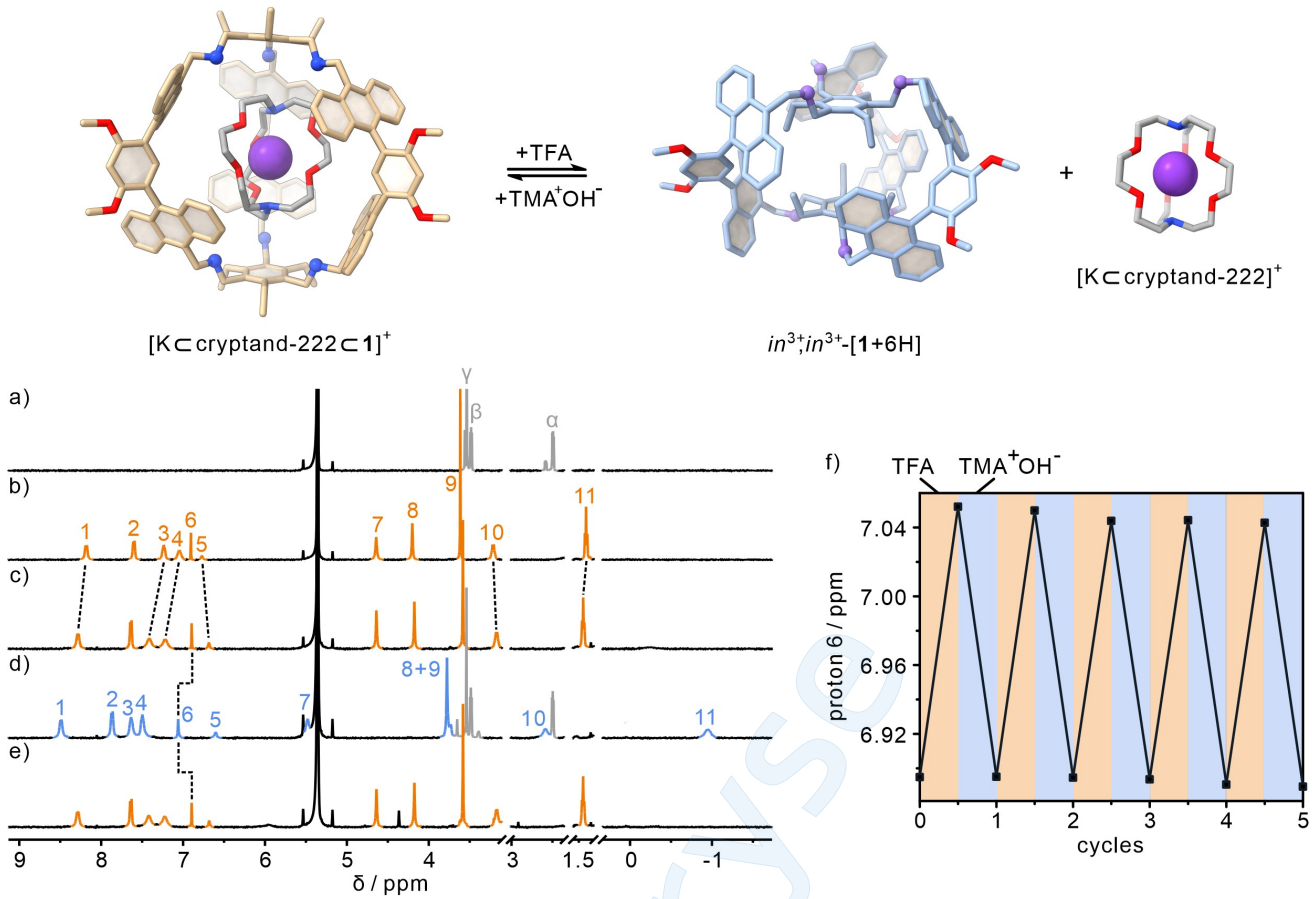

Figure 5. ^{1}H NMR spectra (500 MHz, CD_3CN:CD_2Cl_2 = 1 : 1) of (a) [K⊂cryptand-222]$^+$, (b) cage **1**, (c) [K⊂cryptand-222⊂**1**]$^+$ before and (d) after the addition of TFA (8 molar equiv. based on **1**) and (e) followed by the addition of tetramethylammonium hydroxide (TMA^+OH^-) (8 molar equiv. based on **1**). (f) Chemical shift changes of the proton signal H6 of cage **1** seen upon the sequential addition of TFA and TMA^+OH^-.

6]$^+$ and [K⊂cryptand-222]$^+$). The associated complexation leads to formation of stimuli-responsive Russian doll-like assemblies containing [K⊂18-crown-6⊂**1**]$^+$ and [K⊂cryptand-222⊂**1**]$^+$, respectively. Protonation produces the closed form, [**1**+6H]$^{6+}$, which is ineffective as a receptor. This leads to expulsion of the bound metal complexes. The binding and release process can be switched on and off at will through multiple cycles. The facile synthesis of hexasubstituted benzenes and the ease with which they may be incorporated into environmentally responsive receptor scaffolds leads us to suggest that they could provide the basis for a new class of tunable hierarchical assemblies incorporating on a range of guests. Explorations of this possibility are currently in progress.

Acknowledgements

H.-Y.G. is grateful to the National Natural Science Foundation of China (92156009). X.X. thank the National Natural Science Foundation of China (22274070) and the Shenzhen Municipal Science and Technology Innovation Council (20211029300007) for financial support. We are grateful for the technical support from SUSTech Core Research Facilities and High-Performance Computing services offered by ITS at HKU. The work in Austin was supported by the National Science Foundation (CHE-2304731) and the Robert A. Welch Foundation (F-0018).

Conflict of Interest

The authors declare no conflict of interest.

Data Availability Statement

The data that support the findings of this study are available in the supplementary material of this article.

Keywords: stimuli-responsive systems · Russian doll-like assemblies · molecular cages · host–guest chemistry

[1] a) I. Pochorovski, F. Diederich, *Acc. Chem. Res.* **2014**, *47*, 2096–2105; b) J. S. Park, J. L. Sessler, *Acc. Chem. Res.* **2018**, *51*, 2400–2410; c) A. Blanco-Gómez, P. Cortón, L. Barravecchia, I. Neira, E. Pazos, C. Peinador, M. D. García, *Chem. Soc. Rev.*

2020, *49*, 3834–3862; d) H.-Y. Lin, Y.-T. Wang, X. Shi, H.-B. Yang, L. Xu, *Chem. Soc. Rev.* **2023**, *52*, 1129–1154.
[2] a) E. Benchimol, J. Tessarolo, G. H. Clever, *Nat. Chem.* **2024**, *16*, 13–21; b) A. Ghosh, L. Slappendel, B.-N. T. Nguyen, L. K. S. von Krbek, T. K. Ronson, A. M. Castilla, J. R. Nitschke, *J. Am. Chem. Soc.* **2023**, *145*, 3828–3832; c) S. T. Ryan, J. Del Barrio, R. Suardiaz, D. F. Ryan, E. Rosta, O. A. Scherman, *Angew. Chem. Int. Ed.* **2016**, *55*, 16096–16100; d) K. Kurihara, K. Yazaki, M. Akita, M. Yoshizawa, *Angew. Chem. Int. Ed.* **2017**, *56*, 11360–11364; e) H. Wu, Y. Chen, L. Zhang, O. Anamimoghadam, D. Shen, Z. Liu, K. Cai, C. Pezzato, C. L. Stern, Y. Liu, J. F. Stoddart, *J. Am. Chem. Soc.* **2019**, *141*, 1280–1289; f) X. Chi, W. Cen, J. A. Queenan, L. Long, V. M. Lynch, N. M. Khashab, J. L. Sessler, *J. Am. Chem. Soc.* **2019**, *141*, 6468–6472; g) L. Zhiquan, H. Xie, S. E. Border, J. Gallucci, R. Z. Pavlović, J. D. Badjić, *J. Am. Chem. Soc.* **2018**, *140*, 11091–11100; h) Y. Liu, H. Wang, P. Liu, H. Zhu, B. Shi, X. Hong, F. Huang, *Angew. Chem. Int. Ed.* **2021**, *60*, 5766–5770.
[3] a) J. Yoon, J. Kuwabara, J. H. Kim, C. A. Mirkin, *Science* **2010**, *330*, 66–69; b) N. C. Gianneschi, P. A. Bertin, S. T. Nguyen, C. A. Mirkin, L. N. Zakharov, A. L. Rheingold, *J. Am. Chem. Soc.* **2003**, *125*, 10508–10509.
[4] a) Y.-D. Yang, H.-Y. Gong, *Chem. Commun.* **2019**, *55*, 3701–3704; b) Y. Liu, H. Wang, L. Shangguan, P. Liu, B. Shi, X. Hong, F. Huang, *J. Am. Chem. Soc.* **2021**, *143*, 3081–3085.
[5] Z. Liu, C. Tian, J. Yu, Y. Li, W. Jiang, C. Mao, *J. Am. Chem. Soc.* **2015**, *137*, 1730–1733.
[6] a) G. Hennrich, E. V. Anslyn, *Chem. - Eur. J.* **2002**, *8*, 2218–2224; b) D. J. Iverson, G. Hunter, J. F. Blount, J. R. Damewood, Jr., K. Mislow, *J. Am. Chem. Soc.* **1981**, *103*, 6073–6083; c) K. V. Kilway, J. S. Siegel, *Tetrahedron* **2001**, *57*, 3615–3627.
[7] For selected reviews, see: a) E. Zysman-Colman, C. Denis, *Coord. Chem. Rev.* **2012**, *256*, 1742–1761; b) X. Wang, F. Hof, *Beilstein J. Org. Chem.* **2012**, *8*, 1–10.
[8] For selected molecular cages, see: a) R. A. Tromans, T. S. Carter, L. Chabanne, M. P. Crump, H. Li, J. V. Matlock, M. G. Orchard, A. P. Davis, *Nat. Chem.* **2019**, *11*, 52–56; b) A. P. Bisson, V. M. Lynch, M.-K. C. Monahan, E. V. Anslyn, *Angew. Chem. Int. Ed.* **1997**, *36*, 2340–2342; c) F. Wang, C. Bucher, Q. He, A. Jana, J. L. Sessler, *Acc. Chem. Res.* **2022**, *55*, 1646–1658; d) H. Xie, T. J. Finnegan, V. W. Liyana Gunawardana, W. Xie, C. E. Moore, J. D. Badjić, *Chem. Commun.* **2022**, *58*, 5992–5995; e) O. Francesconi, A. Ienco, G. Moneti, C. Nativi, S. Roelens, *Angew. Chem. Int. Ed.* **2006**, *45*, 6693–6696; f) T. H. G. Schick, J. C. Lauer, F. Rominger, M. Mastalerz, *Angew. Chem. Int. Ed.* **2019**, *58*, 1768–1773; g) S. Lee, A. Yang, T. P. Moneypenny II, J. S. Moore, *J. Am. Chem. Soc.* **2016**, *138*, 2182–2185.
[9] For selected tripodal receptors, see: a) A. Vacca, C. Nativi, M. Cacciarini, R. Pergoli, S. Roelens, *J. Am. Chem. Soc.* **2004**, *126*, 16456–16465; b) H. Valkenier, C. M. Dias, K. L. Porter Goff, O. Jurcek, R. Puttreddy, K. Rissanen, A. P. Davis, *Chem. Commun.* **2015**, *51*, 14235–14238; c) A. Metzger, V. M. Lynch, E. V. Anslyn, *Angew. Chem. Int. Ed.* **1997**, *36*, 862–865; d) T. D. P. Stack, Z. Hou, K. N. Raymond, *J. Am. Chem. Soc.* **1993**, *115*, 6466–6467.
[10] Scifinder substructure searches were conducted for 1,3,5-trialkylbenzene bearing 2,4,6 substituents of the following type CH_2N–, CH_2O–, CH_2S–, and CH_2Ph–.
[11] a) N. Kishi, Z. Li, K. Yoza, M. Akita, M. Yoshizawa, *J. Am. Chem. Soc.* **2011**, *133*, 11438–11441; b) M. Yoshizawa, L. Catti, *Acc. Chem. Res.* **2019**, *52*, 2392–2404.
[12] H. Zhou, X.-Y. Pang, X. Wang, H. Yao, L.-P. Yang, W. Jiang, *Angew. Chem. Int. Ed.* **2021**, *60*, 25981–25987.
[13] J. J. P. Stewart, *MOPAC, Stewart Computational Chemistry*, Colorado Springs, CO, USA **2016**.
[14] a) A. I. Day, R. J. Blanch, A. P. Arnold, S. Lorenzo, G. R. Lewis, I. Dance, *Angew. Chem. Int. Ed.* **2002**, *41*, 275–277; b) T. Iwanaga, R. Nakamoto, M. Yasutake, H. Takemura, K. Sako, T. Shinmyozu, *Angew. Chem. Int. Ed.* **2006**, *45*, 3643–3647; c) H. Wu, Y. Wang, L. O. Jones, W. Liu, B. Song, Y. Cui, K. Cai, L. Zhang, D. Shen, X. Y. Chen, Y. Jiao, C. L. Stern, X. Li, G. C. Schatz, J. F. Stoddart, *J. Am. Chem. Soc.* **2020**, *142*, 16849–16860.
[15] a) S.-Y. Kim, I.-S. Jung, E. Lee, J. Kim, S. Sakamoto, K. Yamaguchi, K. Kim, *Angew. Chem. Int. Ed.* **2001**, *40*, 2119–2121; b) T. Kawase, K. Tanaka, N. Shiono, Y. Seirai, M. Oda, *Angew. Chem. Int. Ed.* **2004**, *43*, 1722–1724; c) D. Zhang, T. K. Ronson, J. L. Greenfield, T. Brotin, P. Berthault, E. Leonce, J. L. Zhu, L. Xu, J. R. Nitschke, *J. Am. Chem. Soc.* **2019**, *141*, 8339–8345; d) L. Zhiquan, S. Polen, C. M. Hadad, T. V. RajanBabu, J. D. Badjic, *J. Am. Chem. Soc.* **2016**, *138*, 8253–8258.
[16] a) T. Sawada, H. Hisada, M. Fujita, *J. Am. Chem. Soc.* **2014**, *136*, 4449–4451; b) S. A. Rousseaux, J. Q. Gong, R. Haver, B. Odell, T. D. Claridge, L. M. Herz, H. L. Anderson, *J. Am. Chem. Soc.* **2015**, *137*, 12713–12718.
[17] K. Cai, M. C. Lipke, Z. Liu, J. Nelson, T. Cheng, Y. Shi, C. Cheng, D. Shen, J. M. Han, S. Vemuri, Y. Feng, C. L. Stern, W. A. Goddard III, M. R. Wasielewski, J. F. Stoddart, *Nat. Commun.* **2018**, *9*, 5275.
[18] a) E. Ubasart, O. Borodin, C. Fuertes-Espinosa, Y. Xu, C. Garcia-Simon, L. Gomez, J. Juanhuix, F. Gandara, I. Imaz, D. Maspoch, M. von Delius, X. Ribas, *Nat. Chem.* **2021**, *13*, 420–427; b) F. M. Steudel, E. Ubasart, L. Leanza, M. Pujals, T. Parella, G. M. Pavan, X. Ribas, M. von Delius, *Angew. Chem. Int. Ed.* **2023**, *62*, e20230939.
[19] a) S. Kamitori, K. Hirotsu, T. Higuchi, *J. Am. Chem. Soc.* **1987**, *109*, 2409–2414; b) T. N. Parac, M. Scherer, K. N. Raymond, *Angew. Chem. Int. Ed.* **2000**, *39*, 1239–1242; c) A. Lützen, A. R. Renslo, C. A. Schalley, B. M. O'Leary, J. Rebek, Jr., *J. Am. Chem. Soc.* **1999**, *121*, 7455–7456; d) N. Grabicki, K. T. D. Nguyen, S. Weidner, O. Dumele, *Angew. Chem. Int. Ed.* **2021**, *60*, 14909–14914; e) Y. Fan, J. He, L. Liu, G. Liu, S. Guo, Z. Lian, X. Li, W. Guo, X. Chen, Y. Wang, H. Jiang, *Angew. Chem. Int. Ed.* **2023**, *62*, e202304623.
[20] Y. Wang, B. Li, J. Zhu, W. Zhang, B. Zheng, W. Zhao, J. Tang, X.-J. Yang, B. Wu, *Angew. Chem. Int. Ed.* **2022**, *61*, e202201789.
[21] S. Mecozzi, J. Rebek, Jr., *Chem. - Eur. J.* **1998**, *4*, 1016–1022.
[22] Deposition numbers 2283985 (for **1**), 2284005 (for in^{3+},in^{3+}-[**1**+6H] $\cdot 6CF_3COO^-$), 2284006 (for in^{3+},out^{3+}-[**1**+6H] $\cdot 6CF_3COO^-$), 2284010 (for $[K\subset 18\text{-crown-}6\subset \mathbf{1}]^+\cdot PF_6^-$), and 2284011 (for $[K\subset \text{cryptand-}222\subset \mathbf{1}]^+\cdot PF_6^-$) contain the supplementary crystallographic data for this paper. These data are provided free of charge by the joint Cambridge Crystallographic Data Centre and Fachinformationszentrum Karlsruhe Access Structures service.

Manuscript received: April 24, 2024
Accepted manuscript online: June 13, 2024
Version of record online: ■■, ■■

Research Article

Host-Guest Systems

X.-Y. Pang, H. Zhou, X. Xie, W. Jiang, Y. Yang, J. L. Sessler,* H.-Y. Gong* **e202407805**

1,3,5–2,4,6-Functionalized Benzene Molecular Cage: An Environmentally Responsive Scaffold that Supports Hierarchical Superstructures

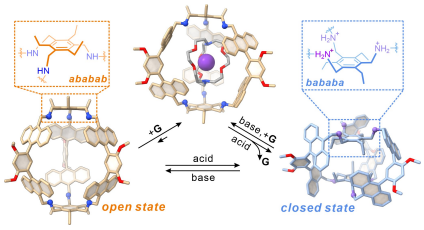

This study presents the first example of a hexasubstituted benzene acting as a switchable motif within a cage-like scaffold. The pH-induced *ababab*↔*bababa* isomerization of the benzene units enables the cage to convert reversibly between an open state and a closed form. The cage was used to create stimuli-responsive Russian doll-like ensembles with $[K\subset 18\text{-crown-6}]^+$ and $[K\subset \text{cryptand-222}]^+$, whose assembly and disassembly could be readily controlled.